

## A THEORETICAL STUDY ON THE MOLECULAR STRUCTURE AND VIBRATIONAL (FT-IR AND FT-RAMAN) SPECTRA OF DIMETHYL QUINOXALINE

T.CHITHAMBARATHANU, M.DARATHI, J.DAISYMAGDALINE

**Abstract:** Combined experimental and theoretical studies have been performed on the structure and the vibrational spectra of the heterocyclic compound dimethyl quinoxaline. Density functional theory (DFT) B<sub>3</sub>LYP calculations have been employed with the standard 6-311++G(d,p) basis set for investigating structural and spectroscopic properties. The vibrational spectra are interpreted with the aid of normal coordinate analysis based on a scaled quantum mechanical forcefield. The calculated HOMO and LUMO energies showed that charge transfer had occurred within the molecule. The Molecular Electrostatic Potential (MESP) analysis reveals the sites for electrophilic attack and nucleophilic reactions in the molecule. Several thermodynamic properties are performed by DFT method. The intra molecular contacts have been interpreted using Natural Bond Orbital analysis.

**Keywords** - DFT, HOMO, LUMO, MESP.

**Introduction:** Quinoxaline and its derivatives are an important class of benzoheterocycles displaying a broad spectrum of biological activities which have made them privileged structures in pharmacologically active compounds. They are important nitrogen containing heterocyclic compounds of various biologically interesting properties with several pharmaceutical applications. Quinoxaline derivatives have antidepressant [1], anticancer [2], antidiabetic [3], anti-inflammatory [4], antimicrobial [5], antiviral [6], antihyperglycemic [7] anti-microbacterial [8] activities and antitumoral properties [9]. Quinoxaline structure acts as a precursor to assemble a large number of new compounds for diverse applications [10]. They are important in industry due to their ability to inhibit the metal corrosion [11-13], in the preparation of the porphyrins, since their structure is similar to the chromophores in the natural system, and also in the electroluminescent materials [14]. Recently, quinoxaline and its analogs have been investigated as the catalyst's ligands [15].

Quinoxalines also have been used as a pigment in the technology of organic dyes [16]. Some of the colour causing substances are reactive dyes that show good stability in cold alkaline solution and have high reactivity such as red Di-Chloro Quinoxaline [17]. But in this industry Quinoxaline has been used as a catalyst and as an agent of reducing azo dyes. Quinoxaline acts like building blocks in the synthesis of anion recipient, DNA fragmentation and the chemical switch control [18-20]. They are also used in agricultural field and cosmetics [21-23]. In the present study, density functional theory (DFT) [24] computations are employed to get insight into the normal modes of dimethyl quinoxaline (DMQ) using Gaussian 03W program package employing 6-311++G(d, p) basis set.

**Experimental details:** Pure spectroscopic Sample of Dimethyl quinoxaline (DMQ) is purchased and used

as such without further purification to record FT-IR and FT-Raman spectra. The FT-IR spectrum of the title compound is measured in the 4000-450 cm<sup>-1</sup> region at a resolution of  $\pm 4$  cm<sup>-1</sup> using Perkin Elmer RXI spectrometer with samples in the KBr. The FT-Raman spectrum is recorded in the 4000-50 cm<sup>-1</sup> Stokes region using Bruker RFS 100/s FT-Raman spectrophotometer with a 1064 nm Nd: YAG laser source of 150 mW power. The spectral resolution is  $\pm 2$  cm<sup>-1</sup>.

**Computational methods:** The quantum chemical calculations have been performed at DFT (B<sub>3</sub>LYP) with 6-311++G (d, p) basis set using Gaussian 03W program [25]. The optimized structural parameters have been evaluated for the calculations of vibrational frequencies. A complete vibrational analysis of the molecule is performed by combining the experimental and theoretical information using Pulay's DFT based scaled quantum mechanical (SQM) approach. Transformations of the forcefield and the subsequent normal coordinate analysis including the least square refinement of scaling factors, calculation of potential energy distribution (PED) and the prediction of IR and Raman intensities have been done on a PC with the MOLVIB program written by Sundius [26]. The redistribution of electron density in various bonding, anti bonding orbitals and E(2) energies have been calculated by Natural Bond Orbital (NBO) analysis to give clear evidence of stabilization originating from the hyperconjugation of various intra-molecular interactions. The HOMO and LUMO analyses have been used to elucidate information regarding charge transfer within the molecule. To investigate the reactive sites of the title compounds, molecular electrostatic potentials are evaluated. Moreover, the thermodynamic parameters at different temperatures ranging from 100 to 1000K are also determined.

**Results and discussions: Molecular Geometry:** The optimized structural parameters of the molecule

under investigation calculated at the B<sub>3</sub>LYP/ 6-311++G (d, p) level is listed in the Table I in accordance with the atom numbering scheme in Fig.1.

Molecular geometries can be specified in terms of bond lengths and bond angles. From the Table 1, it is noted that the ring C<sub>2</sub>-C<sub>3</sub> bond length (1.445Å) in pyrazine ring elongates due to the substitution of methyl groups at C<sub>2</sub> and C<sub>3</sub> for the title compound. C.C.Sangeetha et al. have reported the ring C<sub>2</sub>-C<sub>3</sub> bond length of pyrazine ring as 1.420 Å for the unsubstituted quinoxaline compound [27]. In DMQ, the C<sub>2</sub>- N<sub>1</sub> and C<sub>3</sub>- N<sub>4</sub> bond lengths are calculated as 1.313Å at B<sub>3</sub>LYP/6-311++G (d, p) basis set. Due to the delocalization of electrons present in the methyl groups are wider (118.03°) due to the substitution of methyl group at the position of C<sub>2</sub> and C<sub>3</sub>. On the benzene

group into the ring, the corresponding C-N bond lengths are reduced to 1.313Å from the normal C=N bond length (1.33 Å) [28]. Serdar Badoglu et al. have assigned the C-N bond length as 1.31 Å for the compound 3-hydroxy -2-quinoxaline carboxylic acid [29]. For DMQ, the C-H bond lengths for the ring and methyl group are calculated as 1.084 Å and 1.095 Å by B<sub>3</sub>LYP /6-311++G (d,p) method. Substitution with methyl group leads to some changes of the bond angles in the pyrazine ring. C.C.Sangeetha et al. have reported the C<sub>2</sub>-N<sub>1</sub>-C<sub>10</sub> and C<sub>3</sub>-N<sub>4</sub>-C<sub>5</sub> as 116.53° for the unsubstituted quinoxaline compound [27]. For the title molecule, it is observed that the bond angles C<sub>2</sub>-N<sub>1</sub>-C<sub>10</sub> and C<sub>3</sub>-N<sub>4</sub>-C<sub>5</sub> of the pyrazine ring, the bond angles are smaller or equal typical hexagonal angle of 120°.

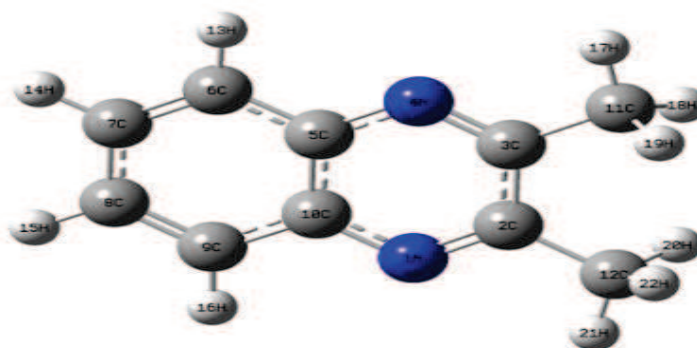


Fig.1 Optimized structure of DMQ

Table I :Optimized geometrical parameters of DMQ obtained by B<sub>3</sub>LYP/6-311++G(d,p).

Bond length <sup>a</sup>	Value(Å)	Bond angle <sup>a</sup>	Value(°)
N <sub>1</sub> -C <sub>2</sub>	1.313	C <sub>2</sub> -N <sub>1</sub> -C <sub>10</sub>	118.03
N <sub>1</sub> -C <sub>10</sub>	1.363	N <sub>1</sub> -C <sub>2</sub> -C <sub>3</sub>	121.36
C <sub>2</sub> -C <sub>3</sub>	1.445	N <sub>1</sub> -C <sub>2</sub> -C <sub>12</sub>	117.73
C <sub>2</sub> -C <sub>12</sub>	1.505	C <sub>3</sub> -C <sub>2</sub> -C <sub>12</sub>	120.91
C <sub>3</sub> -N <sub>4</sub>	1.313	C <sub>2</sub> -C <sub>3</sub> -N <sub>4</sub>	121.36
C <sub>3</sub> -C <sub>11</sub>	1.505	C <sub>2</sub> -C <sub>3</sub> -C <sub>11</sub>	120.89
N <sub>4</sub> -C <sub>5</sub>	1.363	N <sub>4</sub> -C <sub>3</sub> -C <sub>11</sub>	117.74
C <sub>5</sub> -C <sub>6</sub>	1.415	C <sub>3</sub> -N <sub>4</sub> -C <sub>5</sub>	118.03
C <sub>5</sub> -C <sub>10</sub>	1.423	N <sub>4</sub> -C <sub>5</sub> -C <sub>6</sub>	119.89
C <sub>6</sub> -C <sub>7</sub>	1.376	N <sub>4</sub> -C <sub>5</sub> -C <sub>10</sub>	120.61
C <sub>6</sub> -H <sub>13</sub>	1.084	C <sub>6</sub> -C <sub>5</sub> -C <sub>10</sub>	119.49
C <sub>7</sub> -C <sub>8</sub>	1.416	C <sub>5</sub> -C <sub>6</sub> -C <sub>7</sub>	119.90
C <sub>7</sub> -H <sub>14</sub>	1.084	C <sub>5</sub> -C <sub>6</sub> -H <sub>13</sub>	118.16
C <sub>8</sub> -C <sub>9</sub>	1.376	C <sub>7</sub> -C <sub>6</sub> -H <sub>13</sub>	121.94
C <sub>8</sub> -H <sub>15</sub>	1.084	C <sub>6</sub> -C <sub>7</sub> -C <sub>8</sub>	120.60
C <sub>9</sub> -C <sub>10</sub>	1.416	C <sub>6</sub> -C <sub>7</sub> -H <sub>14</sub>	119.96
C <sub>9</sub> -H <sub>16</sub>	1.084	C <sub>8</sub> -C <sub>7</sub> -H <sub>14</sub>	119.44
C <sub>11</sub> -H <sub>17</sub>	1.089	C <sub>7</sub> -C <sub>8</sub> -C <sub>9</sub>	120.60

C11-H18	1.095	C7-C8-H15	119.44
C11-H19	1.095	C9-C8-H15	119.96
C12-H20	1.095	C8-C9-C10	119.90
C12-H21	1.089	C8-C9-H16	121.94
C12-H22	1.095	C10-C9-H16	118.16
-	-	N1-C10-C5	120.61
-	-	N1-C10-C9	119.89
-	-	C5-C10-C9	119.49

<sup>a</sup>atom numbering as in Fig.1.

**Vibrational assignments:** Normal coordinate analysis has been carried out to provide a complete assignment of the fundamental vibrational frequencies for the molecule. A set of local symmetry coordinates are constructed by suitable linear combination of internal coordinates following the recommendations of Fogarasi et al. [30]. The detailed

vibrational analysis of fundamental modes of DMQ along with the FT-IR and FT-Raman experimental frequencies using B3LYP/ 6-311++G (d, p) basis set is presented in Table II. A combined experimental and theoretical spectrum of the title compound has been shown in Fig.2 and Fig.3.

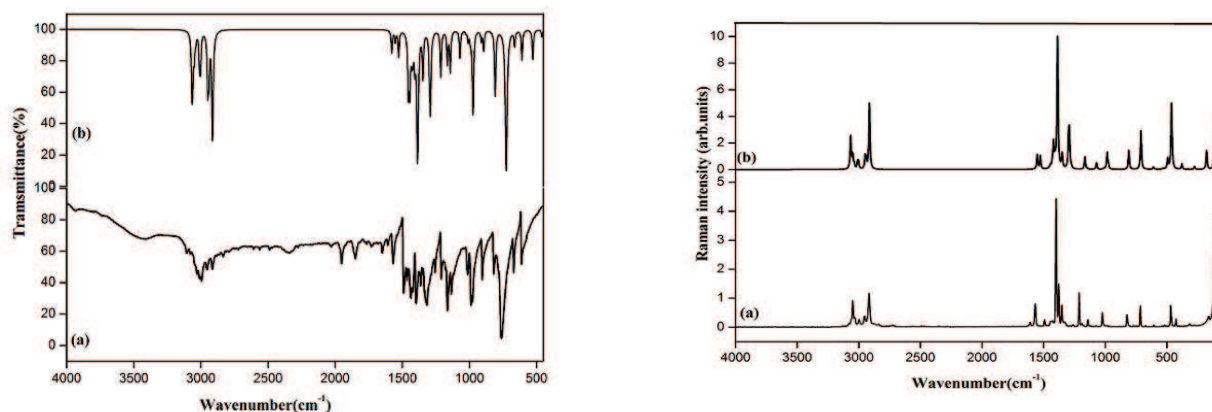


Fig.2 ,3 FT-IR and FT-Raman spectrum of DMQ

Table II: Assignments of fundamental vibrations of DMQ by normal coordinate analysis on SQM force field calculations using selectively scaled B3LYP/6-311++G(d,p).

Observed wavenumber (cm <sup>-1</sup> )		Calculated wave number (cm <sup>-1</sup> ) using B3LYP/ 6-311++G(d,p)	IR Intensity <sup>a</sup>	Raman activity <sup>b</sup>	Characterisation of normal modes with PED (%)
FT- IR	FT-Raman				
3069(w)	3066(w)	3067	14.349	331.563	vCH(99)
-	-	3062	11.749	46.665	vCH(99)
3046(w)	3049(vs)	3050	5.846	136.182	vCH(99)
3038(m)	3037(w)	3037	1.705	50.929	vCH(99)
3010(s)	-	3010	7.954	69.292	CH <sub>30ps</sub> (72)CH <sub>3ips</sub> (19)
2994(s)	2998(m)	3003	8.631	66.060	CH <sub>3ips</sub> (89)CH <sub>3SS</sub> (10)
2954(vs)	2954(m)	2949	15.715	113.715	CH <sub>30ps</sub> (99)

-	-	2940	11.405	82.611	CH <sub>3ips</sub> (76) CH <sub>3ops</sub> (23)
2914(vs)	2916(vs)	2914	39.077	586.645	CH <sub>3ss</sub> (90)
-	2905(w)	2911	1.318	33.011	CH <sub>3ss</sub> (89)
1567(vs)	1568(vs)	1581	5.241	0.005	vCN (46) vCC (23)
-	1556(w)	1555	2.512	32.991	vCC(42) vCN(25)
1536(w)	1534(w)	1531	6.146	29.749	vCC(38) CH <sub>3opb</sub> (27)
1516(w)	-	1526	16.832	2.087	CH <sub>3opb</sub> (76) vCC(12)
1498(vs)	1492(m)	1513	10.036	3.940	CH <sub>3opb</sub> (66) vCC(17)
1464(s)	1468(w)	1449	16.311	6.226	CH <sub>3ipb</sub> (59) vCC(16)
1436(vs)	-	1436	5.05	8.094	CH <sub>3ipb</sub> (65) vCC(32)
-	1428(w)	1424	4.203	22.621	vCN(21) βCH(19)
1399(vs)	1399(vs)	1416	1.365	30.739	vCC (27) CH <sub>3ipb</sub> (24)
-	1377(m)	1389	7.268	15.999	vCC (30)vCN(27)
1363(s)	1353(s)	1351	0.041	22.914	CH <sub>3sb</sub> (74) vCN(13)
1348(m)	-	1347	11.749	4.896	CH <sub>3sb</sub> (82) vCC <sub>ar</sub> (10)
1317(vs)	-	1298	6.752	47.390	vCC (56) vCN (20)
-	1281(w)	1290	23.823	54.361	vCC(68) β CH(13)
1255(s)	1257(w)	1274	0.280	1.936	vCN(39) β CH(24)
1207(s)	1211(vs)	1211	11.775	0.039	β CH (38)vCC(31)
1164(vs)	-	1167	7.999	17.911	vCN(46) vCC(32)
1135(s)	1141(m)	1142	10.311	0.776	β CH (27) vCC <sub>ar</sub> (27)
-	1074(w)	1070	3.820	3.572	β CH(66)vCC(21)
1054(w)	-	1068	2.857	4.796	β CH(75)vCC(13)
-	1023(s)	1025	0.484	0.174	CH <sub>3ipr</sub> (45) CH <sub>3opr</sub> (24)
1014(s)	1014(w)	1007	2.211	1.021	CH <sub>3ipr</sub> (42) CH <sub>3opr</sub> (22)
988(s)	-	995	1.743	0.568	CH <sub>3opr</sub> (60) CH <sub>3ipr</sub> (24)
-	983(w)	983	1.377	18.098	vCC (49)β CH(35)
976(m)	966(w)	973	25.647	4.002	CH <sub>3opr</sub> (31) CH <sub>3ipr</sub> (22)
-	933(w)	927	0.000	0.207	γCH(85)τ ring <sub>1</sub> (15)
904(vs)	-	912	2.298	0.399	γCH(88)τ ring <sub>1</sub> (10)
823(vs)	823(s)	815	0.009	0.008	γCH(65)τ ring <sub>1</sub> (29)
819(w)	-	808	18.140	15.636	vCC(62)vCC <sub>ar</sub> (13)
-	-	724	76.915	0.094	γCH(83)
-	715(s)	710	0.471	26.320	vCC (46) vCC <sub>ar</sub> (16)
-	-	598	0.000	0.119	γCC(53)τ ring <sub>2</sub> (37)
494(w)	498(w)	492	0.053	4.069	βCC (38) β ring <sub>1</sub> (37)

-	375(w)	377	4.264	1.430	$\gamma$ CC(45) $\tau$ ring <sub>2</sub> (35)
-	334(w)	328	0.074	0.058	$\gamma$ CC(38) $\tau$ ring <sub>1</sub> (35)
-	275(w)	274	0.838	0.488	$\beta$ CC(83)
-	255(w)	258	3.123	0.010	$\beta$ CC(55) $\beta$ ring <sub>1</sub> (23)
-	161(w)	176	0.072	1.478	tCC (76)
-	104(vs)	110	0.013	0.685	tCC (86) $\tau$ Butt(11)

vs –very strong ; s – strong; m- medium; w – weak; as- asymmetric; ss – symmetric;  $\nu$  – stretching;  $\beta$  –in-plane bending;  $\gamma$  – out-of- plane bending;  $\tau$  – torsion; sci – scissoring; ro – rocking; wag – wagging; tw – twisting; sb – symmetric bending; ips – in-plane stretching; ops – out-of-plane stretching; ipb – in-plane bending; opb – out-of-plane bending; ipr – in-plane rocking; opr – out-of-plane rocking; Butt- Butterfly.

<sup>a</sup>Calculated IR intensities in  $\text{Km.mol}^{-1}$ .<sup>b</sup>Raman activity in  $\text{A}^+ \text{amu}^{-1}$ .<sup>c</sup>Only PED values greater than 10% are given

**C-H Vibrations:** The aromatic compounds exhibit multiple weak bands in the region  $3100 - 3000 \text{ cm}^{-1}$  due to C-H stretching vibrations [31, 32]. In DMQ molecule, the bands at  $3069, 3046, 3038 \text{ cm}^{-1}$  in FT- IR spectrum and the bands at  $3066, 3049, 3037 \text{ cm}^{-1}$  in FT-Raman are assigned to C-H stretching vibrations. The theoretically computed wavenumbers by B<sub>3</sub>LYP/6-311++G (d, p) method are identified at  $3067, 3062, 3050$  and  $3037 \text{ cm}^{-1}$  with PED contribution of 99% and is shown in Table II.

**Methyl group vibrations:** Methyl group vibrations are generally referred to as electron-donating substituent in the aromatic ring system. For the methyl group, the asymmetric stretching vibration is observed in the region  $2940 - 3010 \text{ cm}^{-1}$  and the symmetric stretching appears in the region  $2840 - 2970 \text{ cm}^{-1}$  [36]. The asymmetric stretch is at higher wavenumber than the symmetric stretch. For the title compound, methyl groups are attached to the second and third carbon atom of the pyrazine ring. In DMQ molecule, strong bands at  $3010, 2994, 2954 \text{ cm}^{-1}$  in FT-IR and medium bands at  $2998, 2954 \text{ cm}^{-1}$  in FT-Raman spectrum have been assigned to asymmetric stretching vibrations. The computed wave numbers of the modes corresponding to the asymmetric stretching vibrations of methyl groups are identified at  $3010, 3003, 2949$  and  $2940 \text{ cm}^{-1}$  by B<sub>3</sub>LYP/6-311++G(d, p) method. The observed bands at  $2916, 2905 \text{ cm}^{-1}$  in FT-Raman and a very strong band at  $2914 \text{ cm}^{-1}$  in FT-IR spectrum are attributed to the symmetric stretching vibrations whereas the corresponding theoretical modes of the two methyl groups have been identified at  $2914$  and  $2911 \text{ cm}^{-1}$  respectively.

The C-H in- plane bending vibrations normally occur as a number of strong to weak bands in the region  $1300-1000 \text{ cm}^{-1}$  [33]. In the title molecule, C-H in-plane bending vibrations are identified at  $1211, 1141, 1074 \text{ cm}^{-1}$  in FT-Raman and at  $1207, 1135, 1054 \text{ cm}^{-1}$  in FT-IR spectrum. The theoretically calculated wave numbers at  $1211, 1142, 1070$  and  $1068 \text{ cm}^{-1}$  have been assigned to C-H in- plane bending vibrations. The frequencies of the C-H out-of- plane deformation vibrations are mainly determined by the number of adjacent hydrogen atoms on the ring and normally occurs in the region  $900 - 650 \text{ cm}^{-1}$  [34]. Strong bands at  $904, 823 \text{ cm}^{-1}$  in FT-IR and bands at  $933, 823 \text{ cm}^{-1}$  in FT-Raman spectrum have been assigned to C-H out-of-plane ring deformation vibrations respectively. The C-H out-of-plane ring deformation vibrations of DMQ are identified at  $927, 912, 815$  and  $724 \text{ cm}^{-1}$  by B<sub>3</sub>LYP/6-311++G (d, p) method. The computed as well as the recorded spectral data are found to match very well with the literature [35].

The asymmetric deformations of the methyl groups are expected in the region  $1445 \pm 25 \text{ cm}^{-1}$  [36]. The asymmetrical methyl deformation modes are identified at  $1516, 1498, 1464, 1436 \text{ cm}^{-1}$  in IR and at  $1492, 1468 \text{ cm}^{-1}$  in Raman spectrum. The theoretically calculated values for these modes are observed at  $1526, 1513, 1449$  and  $1436 \text{ cm}^{-1}$ . The symmetric deformations appear in the region  $1380 \pm 20 \text{ cm}^{-1}$  [36]. For DMQ, the symmetrical methyl deformation modes  $\text{CH}_{3\text{sb}}$  of two methyl groups are observed as a strong band at  $1353 \text{ cm}^{-1}$  in Raman and strong and medium bands at  $1363, 1348 \text{ cm}^{-1}$  in the IR spectrum. The DFT calculations give  $1351$  and  $1347 \text{ cm}^{-1}$  as symmetric methyl deformation modes. The methyl in-plane and out-of-plane rocking modes usually appear in the region  $1080 \pm 80 \text{ cm}^{-1}$  and  $1170 \pm 95 \text{ cm}^{-1}$  [36]. The  $\text{CH}_3$  in-plane and out-of-plane rocking modes are observed at  $1023, 1014, 966 \text{ cm}^{-1}$  in Raman and strong bands at  $1014, 998$  and  $976 \text{ cm}^{-1}$  in IR spectrum. The theoretically calculated values corresponding to these modes are identified at  $1025, 1007, 995$  and  $973 \text{ cm}^{-1}$  by B<sub>3</sub>LYP/6-311++G(d, p) method. These assignments are also supported by literature [37].

**C-C vibrations:** The carbon-carbon stretching modes of aromatic ring are usually occurred in the range from 1650- 1200  $\text{cm}^{-1}$ . The actual positions of these modes determined are not affected much by the nature of the substituents, but by the position of the substitution around the ring [38]. N.Prabavathi et al. assigned the skeletal vibrations (ring CC) in the region 1677- 912  $\text{cm}^{-1}$  theoretically for the compound 2-quinoxaline carboxylic acid [35]. In DMQ, the ring

**C-N vibrations:** The C-N stretching frequency is a rather difficult task since the mixing of several bands is possible in this region. Sundaraganesan assigned the band at 1689 and 1302  $\text{cm}^{-1}$  to C=N and C-N stretching vibration respectively for the compound benzimidazole [39]. N.Prabavathi et al. have assigned the bands at 1563 and 1537  $\text{cm}^{-1}$  to C=N vibrations and at C-N stretching 1290 and 1240  $\text{cm}^{-1}$  for the quinoxaline moiety [35]. In the present work, the bands observed at 1568 and 1428  $\text{cm}^{-1}$  in FT-Raman and a very strong band at 1567  $\text{cm}^{-1}$  in IR spectrum have been attributed to C=N vibrations. The theoretically computed value of the corresponding C=N stretching vibrations are predicted at 1581,1424  $\text{cm}^{-1}$ . The peaks identified at 1255 and 1164  $\text{cm}^{-1}$  in IR and 1257  $\text{cm}^{-1}$  in FT-Raman spectrum have been assigned to C-N stretching absorption bands whereas the theoretically computed values are predicted at 1274 and 1167  $\text{cm}^{-1}$ . These vibrations are mixed with C-C stretching as evident from PED.

**Natural bond orbital analysis:** NBO analysis has been performed on dimethyl quinoxaline in order to elucidate intra molecular hydrogen bonding, intramolecular charge transfer (ICT) interactions type and delocalization of  $\pi$  electrons of the ring. In order to investigate the intra and intermolecular interactions, the stabilization energies of the title compound are performed by using second-order perturbation theory. The change in electron density (ED) in the ( $\sigma^*$ ,  $\pi^*$ ) antibonding orbitals and  $E(2)$  energies have been calculated by natural bond orbital analysis [40] using DFT method to give clear evidence of stabilization originating from various molecular interactions. The hyperconjugative interaction

C-C stretching vibrations are identified at 1536, 1399, 1317,1207  $\text{cm}^{-1}$  in FT-IR and at 1556,1534, 1399, 1377, 1281, 983 $\text{cm}^{-1}$  in Raman spectrum. The theoretically calculated wave numbers by B3LYP/6-311++G (d, p) method, are observed at 1555, 1531, 1416, 1389, 1298, 1290 and 983  $\text{cm}^{-1}$ . The C-C in-plane bending and out-of-plane bending modes are associated with smaller force constants than the stretching ones, and hence assigned to lower frequencies.

energy is deduced from the second-order perturbation approach [41]

$$E(2) = \Delta E_{ij} = q_i \frac{F^2(i, j)}{\epsilon_j - \epsilon_i}$$

Where  $q_i$  is the donor orbital occupancy,  $\epsilon_i$  and  $\epsilon_j$  are diagonal elements and  $F(i, j)$  is off-diagonal Fock matrix element. The larger the  $E(2)$  value, the more intensive is the interaction between electron donors and electron acceptors, i.e., the more donating tendency from electron donors and electron acceptors and greater the extent of conjugation of the whole system.

The Fock matrix analysis yields different types of donor-acceptor interactions and their stabilisation energy. All lone pair-bond pair interactions with stabilization energies more than 5  $\text{kcalmol}^{-1}$  are listed in Table III. In DMQ molecule, since methyl group is an electron donating substituent in aromatic ring system, it interacts with nearby  $\pi$ -system via hyper conjugation. The intramolecular hyperconjugative interaction of the  $\pi$  - $\pi^*$  transitions from (C6-C7) to (C5-C10) lead to strong delocalization with stabilization energy of 17.27  $\text{kcalmol}^{-1}$ . The most interaction energy, related to the resonance in the molecule, electron donating from the  $n_1(N_1)$  and  $n_1(N_4)$  to the antibonding  $\sigma^*(C_2-C_3)$  and  $\sigma^*(C_2-C_3)$  leads to moderate stabilization energy of 9.90  $\text{kcalmol}^{-1}$  and 9.93  $\text{kcalmol}^{-1}$  respectively. Another interaction is calculated at  $\pi^*(C_8-C_9)$  to  $\pi^*(C_6-C_7)$  which shows enormous stabilization energy of 244.61  $\text{kcalmol}^{-1}$ .

**Table III: Second order perturbation theory analysis of Fock matrix in NBO basis for DMQ.**

Donor(i)	ED(i) (e)	Acceptor(j)	ED(j) (e)	$E(2)^a$ $\text{kcalmol}^{-1}$	$E(j) - E(i)^b$ (a.u.)	$F(i,j)^c$ (a.u.)
$\pi(N_1-C_2)$	1.78392	$\pi^*(C_3-N_4)$	0.27343	14.35	0.33	0.062
		$\pi^*(C_5-C_{10})$	0.43965	18.34	0.34	0.075
$\pi(C_3-N_4)$	1.78393	$\pi^*(C_5-C_{10})$	0.43965	18.34	0.34	0.075

$\pi(C5-C10)$	1.51674	$\pi^*(N1-C2)$	0.27344	14.91	0.27	0.059
		$\pi^*(C3-N4)$	0.27343	14.91	0.27	0.059
		$\pi^*(C6-C7)$	0.24854	15.41	0.29	0.063
		$\pi^*(C8-C9)$	0.24853	15.41	0.29	0.063
$\pi(C6-C7)$	1.73144	$\pi^*(C5-C10)$	0.43965	17.27	0.28	0.065
		$\pi^*(C8-C9)$	0.24853	17.41	0.29	0.064
$\pi(C8-C9)$	1.73145	$\pi^*(C5-C10)$	0.43965	17.27	0.28	0.065
		$\pi^*(C6-C7)$	0.24854	17.41	0.29	0.064
$n1(N1)$	1.92637	$\sigma^*(C2-C3)$	0.05460	9.90	0.85	0.082
		$\sigma^*(C5-C10)$	0.04979	8.73	0.89	0.034
$n1(N4)$	1.92625	$\sigma^*(C2-C3)$	0.05460	9.93	0.85	0.082
		$\sigma^*(C5-C10)$	0.04979	8.74	0.89	0.079
$\pi^*(C8-C9)$	0.43965	$\pi^*(C6-C7)$	0.24854	244.61	0.01	0.079
		$\pi^*(C8-C9)$	0.24853	244.56	0.01	0.079

<sup>a</sup> E(2) means energy of hyper conjugative interactions.

<sup>b</sup> Energy difference between donor and acceptor i and j NBO orbitals

<sup>c</sup> F(i,j) is the Fock matrix element between i and j NBO orbital

**Frontier molecular orbitals:** The frontier molecular orbitals not only determine the way the molecule interacts with other species, but their energy gap (frontier orbital gap) helps to characterize the chemical reactivity and kinetic stability of the molecule. The HOMO is the orbital that primarily acts as an electron donor (Highest occupied MO) and LUMO is the orbital that largely acts as the electron acceptor (Lowest unoccupied MO) and the gap between HOMO and LUMO characterizes the molecular chemical stability. The energy gap between the highest occupied and the lowest unoccupied molecular orbital, is a critical parameter in determining molecular electrical transport properties

because it is a measure of electron conductivity. Fig.4. Shows the distributions and energy levels of the HOMO and LUMO orbitals computed at the B3LYP/6-311++G (d, p) level for the title compound. The value of the energy separation between the HOMO-LUMO is found to be 0.17956 a.u. The dipole moment reflects the molecular charge distribution. Therefore, it can be used as descriptor to depict the charge movement across the molecule. The calculated dipole moment values for the molecule is also given in Table IV. The bigger the dipole moment, the stronger will be the intermolecular interactions. The dipole moment of DMQ is found to be 0.7481 Debye.

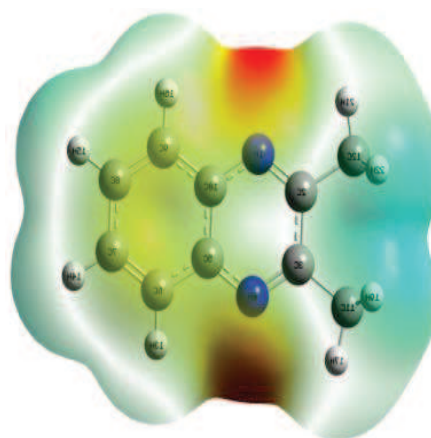
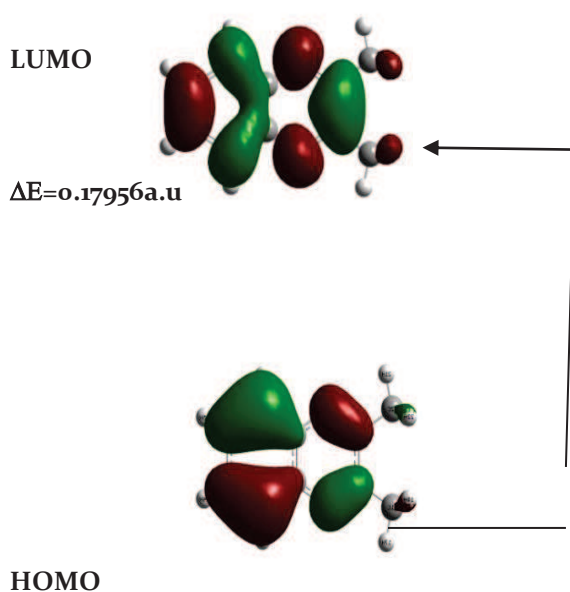


Fig4. Frontier molecular orbitals of DMQ

Fig.5 Molecular Electrostatic Potential of DMQ

**Molecular electrostatic potential (MESP):** The molecular electrostatic potential (MESP) is used primarily for predicting sites and relative reactivities towards electrophilic attack, in studies of biological recognition and hydrogen bonding interactions [42,43]. To predict the reactive sites of electrophilic and nucleophilic attack for the investigated molecule, the MESP at the B<sub>3</sub>LYP/6-311++ G(d, p) optimized geometry is calculated and shown in Fig. 5. The negative (red) regions of MESP are related to electrophilic reactivity and the positive (blue) regions are related to nucleophilic reactivity. The MESP map shows that in DMQ, the negative potentials are over the electronegative nitrogen atom in the pyrazine ring. In addition, the positive potential sites around the hydrogen atoms of methyl group indicates that these sites are involved in nucleophilic processes. However, the H atoms in the ring have higher positive potential than the H atoms in the methyl group. Red and blue areas in the MESP map refer to the regions of negative and positive potential and correspond to the electron rich and electron-poor region, respectively, whereas the green colour signifies the neutral electrostatic potential. (0.99931)

**Thermodynamic properties:** The variation in Zero-Point Vibrational Energies (ZPVEs) seems to be significant. The values of some thermodynamic parameters such as zero-point vibrational energy, rotational constant, and dipole moment of DMQ at 298.150 K and 1.00 atm pressure are listed in Table IV. On the basis of vibrational analysis at B<sub>3</sub>LYP/6-311++G(d, p) level, the standard statistical thermodynamic functions: heat capacity (C), entropy (S), and enthalpy changes (H) are obtained from the theoretical harmonic frequencies and are listed in the Table V. It is observed that the thermodynamic functions are increasing with temperature ranging from 100 to 1000 K due to the fact that the molecular vibrational intensities increase with temperature [44]. The correlation equation between heat capacities, entropies, enthalpy changes and temperatures are fitted by quadratic formulas and the corresponding fitting equations, fitting factors (R<sup>2</sup>) for these thermodynamic properties for the title compound are given below.

For dimethyl quinoxaline,

$$S = 52.3109 + 0.15942T - 3.1256 \times 10^{-5}T^2 \quad (R^2 = 0.99999)$$

$$C_p = 0.22723 + 0.15955T - 6.3656 \times 10^{-5}T^2 \quad (R^2 =$$

$$H = -1.66083 + 0.01639T + 4.50115 \times 10^{-5}T^2 \quad (R^2 = 0.9995)$$

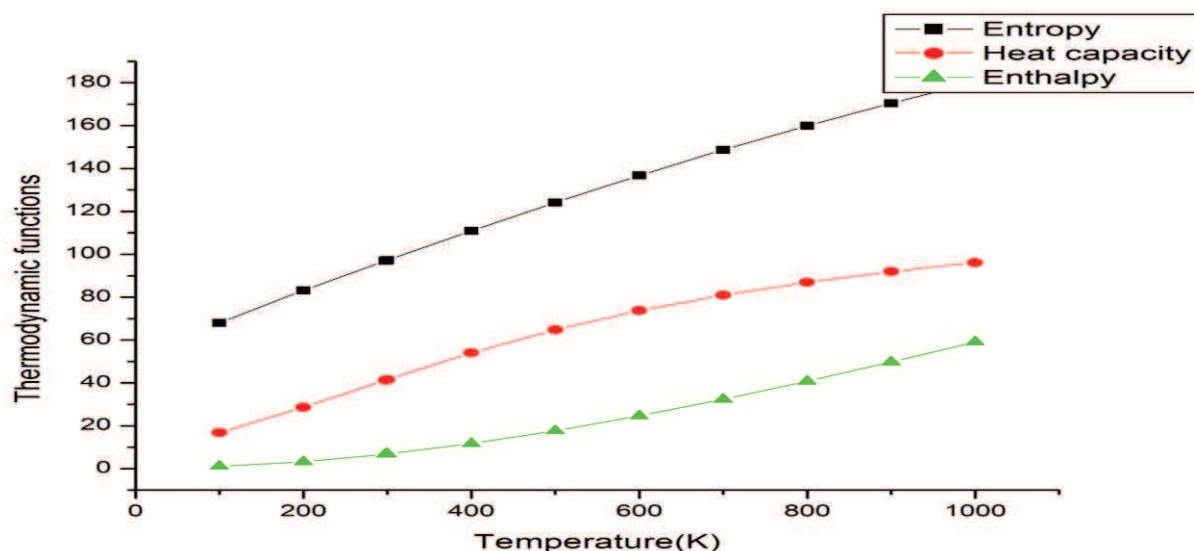


Fig. 6 Correlation graph of thermodynamic function and temperature for DMQ



Table IV: Theoretically computed zero point vibrational energy, rotational constants and dipole moment

Temperature (K)	Entropy (S) cal/mol-K	Heat capacity ( $C_p$ ) cal/mol-K	Enthalpy ( $\Delta H_m$ ) k cal/mol
100	67.947	16.812	1.146
200	83.170	28.680	3.208
298.15	96.959	41.311	6.841
300	97.215	41.551	6.918
400	110.907	54.029	11.707
500	124.160	64.829	17.667
600	136.792	73.712	24.610
700	148.718	80.963	32.357
800	159.932	86.938	40.762
900	170.468	91.921	49.713
1000	180.376	96.119	59.122

Table V: Thermodynamic Properties of DMQ

Thermodynamic parameters	DMQ
Total energy(thermal)kcal/mol	117.707
Vibrational energy kcal/mol	115.930
Zeropoint Vibrational energy kcal/mol	111.459
Rotational constants(GHz)	
A	2.182
B	0.714
C	0.541
Dipole moment	
$\mu_x$	0.748
$\mu_y$	0.0001
$\mu_z$	0.357
$\mu_{total}$	0.829

**Conclusion:** FT-IR and FT-Raman spectra of dimethyl quinoxaline are recorded and the detailed vibrational assignments have been obtained. The molecular geometry, vibrational frequencies, infrared intensities and Raman scattering activities of the molecule is calculated by using B3LYP/6-311++G (d, p) method. All the vibrational frequencies are calculated and scaled values are compared with experimental FT-IR and FT-Raman spectra. The observed and the

calculated frequencies are in good agreement. The influence of methyl group in the title compound is discussed. The MESP map shows that the negative regions are mainly localized on the electronegative atoms while the maximum positive region is localized on the methyl group. These sites give information about the region where the compound can have intramolecular interactions. In addition, the energy gap between the HOMO-LUMO is calculated. The

NBO analysis revealed that the  $\pi$ - $\pi^*$  interaction gives the strongest stabilization energy to the system. The correlation between the statistical thermodynamics

and temperature are also obtained. It has been observed that the heat capacities, entropies and enthalpies increase with increasing temperature.

### References:

1. R.Sarges, H.R.Howard, R.G.Browne, L.A.Lebel, P.A.Seymour, B.K.Koe, *J.Med.Chem.*, 33(1990)2240.
2. H.W.Yoo, M.E.Suh, S.W.Park, *J.Med.Chem.*, 41 (1998).
3. M.Y.Chu Moyer, W.E.Ballinger, D.A.Beebe, R.Berger, J.B.Coutcher, W.W.Day, J.Li, B.L.Milari, P.J.Oates, R.M.Weekly, *J.Med. Chem.*, 45 (2002) 511
4. C.V.Reddy Sastry, K.S.Rao, V.S.H.Krishnan, K.Rastogi, M.L.Jain, G.K.A.S.S.Narayan, *Indian J.Chem.*, 29(1990) 396.
5. I.M.A.Awad, *IndiaChem.*, 30 (1991) 89.
6. Z.Zhu, S.Saluja, J.C.Drach, L.B.Townsend, *J.Chin.Chem.Soc.*, 45 (1998) 4651.
7. P.Y.Pawar, S.B.Bhise, *Indian J. Physiol, Pharmacol.*, 50 (2006) 431.
8. E.S.Lainne, J.S.William, C.R.Robert, *J.Med.Chem.*, 45 (2002) 5604.
9. J.Renault, Michel Baron, Patrick Mailliet et al. *Eur.J. Med. Chem.*, 16 (1981) 545.
10. Y. Deepika, P.N., K. Sachin, S. Shewta, *Int. J. Curr. Pharm. Rev. Res.*, 1(3) (2011) 33.
11. Z. El Adnani, M. M, M. Sfaira, M. Benzakour, A. Benjelloun, M. EbnTouhami, B. Hammouti, M. Taleb, *Int. J. Electrochem.Sci.*, 7 (2012) 13.
12. I.B. Obot, N.O. Obi-Egbedi, *Corrosion Science* 52(1) (2010).
13. J.A. Pereira et al., *Eur.J. Med. Chem.*, (2014).
14. K.R. Justin Thomas, M. V., Jiann T. Lin, Chang-HaoChuen, Yu-Tai Tao, *Chem. Mater.*, 17 (2005).
15. Xianghong Wu, Anne E.V. Gorden. *J.Org. Chem.*, 72 (2007).
16. E.D. Brock, D.M. Lewis, T.I. Yousaf, H.H. Harper, The Procter & Gamble Company, USA WO, 1999.
17. Dytner, E. Finimore, U. Meyer, *J. Soc. Dyers Colour*, 1997.
18. Jaso, B. Zarranz, I. Aldana, A. Monge, *Eur. J. Med. Chem.*, (2003).
19. L.S. Jonathan, M. Hiromitsu, M. Toshihisa, M.L. Vincent, F.J. Hiroyuki, *Chem. Commun.*, (2002) 13474.
20. P.C. Peter, Z. Gang, A.M. Grace, H. Carlos, M.G.T. Linda, *Org. Lett.*, (2004) 333.
21. Y.Ikeda, E.Kuwano, M.Eto, *J.Fac.Agric.*, 37(1992)81.
22. Y.Laura, G.Sakata, K.Makino, T.Ikai, Y.Kawamura, *German Offenlegungschrift, Org. Lett.*, 6 (2004).
23. N.T.Ghoms, N.H.Ahabchane, N.Es.Safi, B.Garrigues, E.M.Essasi *Spectrosc.Lett.*, 40(2007)741.
24. P.Hohenberg, W.Kohn, *Phys.Rev.*, 136(1964) 864.
25. M.J.Frisch et al., Gaussian 03 program, Gaussian Inc Wallingford, CT 2004.
26. T.Sundius, MOLVIB(v.7.0), Calculation Force Fields and Vibrational Modes of Molecules, *Vib.Spectrosc.*, 29 (2002)89.
27. C.C.Sangeetha, R.Madivanane, V.Pouchaname, *Int.J. Chem. Tech. Res.*, (2014) 2854.
28. V.Arjunan et al., *Spectrochimica Acta Part A: Molecular and Biomolecular Spectroscopy* 96 (2012) 506.
29. S.Badoglu, S.Yurdakul, *Spectrochimica Acta A: Molecular and Biomolecular Spectroscopy* 101(2013) 14.
30. P.Pulay, G.Forgrasi, G.Pongor, J.E.Boggs, A.Varga, *J.Am. Chem.Soc.*, 105. (1983)7037.
31. W.O.George, P.S.Mcintyre, *Infrared spectroscopy*, John Wiley & Sons London 1987.
32. L.G.Socrates, *Infrared and Raman characteristic Group Frequencies-Tables and charts third ed.*, Wiley, New York, 2001.
33. V.Krishnakumar, N.Prabhavathi *Spectrochimica Acta A* 71 (2008) 449.
34. M.Karabacak et al., *J.Mol.Struct.*, 982(2010) 22.
35. N.Prabhavathi, A.Nilufer, V.Krishnakumar. *Spectrochimica Acta Part A* 92 (2002) 325.
36. N.P.G.Roeges, *A Guide to the Complete Interpretation of the Infrared Spectra of Organic structures*, Wiley, New York, 1974
37. S.J.Bunce, H.G.Edwards, F.Johnson, I.R.Lewis, P.H.Turner *Spectrochim Acta* 49A(1993)77 5.
38. V.Arjunan., *Spectrochimica Acta A Part A : Molecular Biomolecular Spectroscopy* 98 (2012) 156.
39. N.Sundaraganesan, S.Ilakiamani, P.Subramanian, B.D.Joshua *Spectrochimica Acta* 67A (2007) 628.
40. P.Torkington, *J.Chem. Soc.* 36H.W.Thomson, 171(1945) 640.
41. E.D.Glendering, A.E.Reed, J.E.Carpenter, F.Weinhold NBO version 3.1, TCI, University of Wisconsin, Madison, 1998.
42. J.S.Murray, K.Sen, *Molecular Electrostatic Potentials, Concepts and Applications*, Elsevier, Amsterdam, 1996. E. Scrocco, J. Tomasi, *Adv. Quantum Chem.*, 11(1978)115.
43. E. Scrocco, J. Tomasi, *Adv. Quantum Chem.* 11 (1978) 115.
44. J. Bevan Ott, J.Boerio-Goates, *calculations from statistical Thermodynamics Academic Press*, 2004.

\* \*\*

T. Chithambarathanu  
Principal, S.T. Hindu College, Nagercoil  
Manonmaniam Sundaranar University, Tirunelveli. Tamil Nadu

M. Darathi, J. DaisyMagdeline  
Associate Professor of Physics  
Rani Anna Govt College, Tirunelveli  
Manonmaniam Sundaranar University, Tirunelveli, Tamil Nadu